Preparation and Properties of $NbBr_4(PMe_2Ph)_3$ and $NbBr_3(PMe_2Ph)_3$

F. ALBERT COTTON*, MICHAEL P. DIEBOLD and WIESLAW J. ROTH

Department of Chemistry and Laboratory for Molecular Structure and Bonding, Texas A & M University, College Station, Tex. 77843, U.S.A.

Received February 13, 1985

Abstract

Niobium(V) bromide reacts with PMe_2Ph in toluene at 25 °C to give dark red $NbBr_4(PMe_2Ph)_3$, **1**, in 70% isolated yield, excess PMe_2Ph serving as the reducing agent. The molecule has a capped octahedral structure with an uncapped Br_3 face parallel to a Br-capped P_3 face. Mean distances are: Nb–Br(cap) = 2.541(4) Å, Nb–Br(3x) = 2.604[10] Å, and Nb–P(3x) = 2.704[11] Å. Crystals are orthorhombic, *Pnna*, with $a = 14.345(3)$ Å, $b = 41.189(9)$ Å, $c = 9.943(4)$ Å, $V = 5875(5)$ Å^3, $Z = 8$. When the reaction of $NbBr_5$ with excess PMe_2Ph was carried out in presence of one mole of Na/Hg per mole of $NbBr_5$, a >50% yield of red $NbBr_3(PMe_2Ph)_3$, **2**, was obtained. The molecule has a *mer*-octahedral structure with the following mean distances: Nb–Br = 2.573(1) Å, Nb–Br(2x) = 2.558[4] Å, Nb–P = 2.716(2) Å, Nb–P(2x) = 2.633[14] Å. Crystals are triclinic, $P\bar{1}$, with $a = 9.625(3)$ Å, $b = 19.424(5)$ Å, $c = 8.979(2)$ Å, $\alpha = 97.42(2)°$, $\beta = 94.08(2)°$, $\gamma = 98.56(3)°$, $V = 1639(2)$ Å^3, $Z = 2$. The structures of **1** and **2** are compared with those of other $MX_4(PR_3)_3$ and $MX_3(PR_3)_3$ molecules. The EPR spectra are reported and discussed.

Introduction

The stereochemistry and stoichiometry of phosphine adducts of Nb(IV) and Ta(IV) chlorides [1–6] are markedly influenced by the steric requirements of the neutral ligand. Triethylphosphine and those which are larger form *trans* octahedral complexes, MCl_4L_2. When the smaller phosphines PMe_3 or PMe_2Ph are used, the metals usually adopt structures with higher coordination numbers consistent with the smaller steric requirements. The following complexes have been identified: an eight coordinate monomer, $NbCl_4(PMe_3)_4$, eight-coordinate dimers, $M_2Cl_8(PMe_3)_4$, of both elements, $Nb_2Cl_8(PMe_2Ph)_4$, and the seven-coordinate $MCl_4(PMe_3)_3$ compounds of both elements. In addition there is the octahedral complex, *cis*-$TaCl_4(PMe_2Ph)_2$. Knowing the response of the metals to changing size of the phosphine ligand we wanted to examine the effect a larger halide would have on the geometry and we therefore attempted to prepare some niobium bromo derivatives of PMe_2Ph. However, the change from chloride to bromide introduced still another factor because the phosphines can readily reduce $NbBr_5$ to lower oxidation states. In the presence of excess PMe_2Ph the major product is $NbBr_4(PMe_2Ph)_3$, **1**, even when no other reducing agent is present, and $NbBr_3(PMe_2Ph)_3$, **2**, if one equivalent of sodium amalgam is added.

Both compounds possess conventional structures, which are of interest since crystallographic data concerning analogous complexes of other metals are available. There have been indications that phosphine adducts of Nb and Ta have some unexpected metal–ligand bond length relationships. The two species reported here provide a basis for more direct examination of this phenomenon. Another interesting feature of these results is that complex **2** is the first structurally characterized MX_3L_3 monomer of Nb(III) or Ta(III). These elements have a tendency to form dinuclear species with a double metal–metal bond in their +3 oxidation state [7–10]** and only a few monomeric complexes have been reported [8, 11]. It is useful to learn more about such mononuclear species in order to understand better the role of metal–metal bonds in the remarkable reactivity of Nb(III) and Ta(III) dimers [12, 13].

Experimental

Preparations

All manipulations were carried out under an atmosphere of argon. Standard vacuum line techniques were used. Niobium(V) bromide and

*Author to whom correspondence should be addressed.

**Structurally characterized Nb^{III} and Ta^{III} dimers are discussed in ref. 7.

0020-1693/85/$3.30

TABLE I. Crystallographic Data.

	1	2
Formula	$NbBr_4P_3C_{24}H_{33}$	$NbBr_3P_3C_{27\frac{1}{2}}H_{37}$
Formula weight	826.99	793.16
Space group	*Pnna*	$P\bar{1}$
Systematic absences	$0kl$: $k + l = 2n + 1$ $h0l$: $h + l = 2n + 1$ $hk0$: $h = 2n + 1$	
a (A)	14.345(3)	9.625(3)
b (A)	41.189(9)	19.424(5)
c (A)	9.943(4)	8.979(2)
α (deg)	90.0	97.42(2)
β (deg)	90.0	94.08(2)
γ (deg)	90.0	98.56(3)
V (A^3)	5875(5)	1639(2)
Z	8	2
D_{calc} (g/cm^3)	1.871	1.607
Crystal size (mm)	0.3 × 0.25 × 0.07	0.2 × 0.1 × 0.1
μ(Mo Kα) (cm^{-1})	59.572	41.336
Data collection instrument	CAD-4	Syntex $P\bar{1}$
Radiation (monochromated in incident beam)	Mo Kα (λ = 0.71073 Å)	
Orientation reflections, number, range (2θ)	25, 8.0 < 2θ < 23.0	15, 20.3 < 2θ < 31.0
Temperature (°C)	20	5
Scan method	ω	$\omega - 2\theta$
Data col. range, 2θ (deg)	4, 50	
No. unique data, total	2382	4418
with $F_o^2 > 3\sigma(F_o^2)$	1192	3010
Number of parameters refined	169	304
Trans. factors, max, min.	0.9992, 0.6364	0.9997, 0.7698
R[a]	0.068	0.047
R_w[b]	0.069	0.060
Quality-of-fit indicator[c]	1.288	1.193
Largest shift/e.s.d., final cycle	0.26	0.20
Largest peak ($e/Å^3$)	1.059[d]	0.674

[a] $R = \Sigma\|\|F_o| - |F_c\|\|/\Sigma|F_o|$. [b] $R_w = [\Sigma w(|F_o| - |F_c|)^2/\Sigma w|F_o|^2]^{1/2}$; $w = 1/\sigma^2(|F_o|)$. [c] Quality of fit = $[\Sigma w(|F_o| - |F_c|)^2/(N_{obs} - N_{parameters})]^{1/2}$. [d] In the proximity of the Nb atom.

dimethylphenylphosphine were purchased from Aldrich and Strem Chemicals, Inc., respectively, and used as received. EPR and NMR spectra were recorded on an X-band Varian E-6S and EM390 spectrometers, respectively. Elemental analyses were done by Galbraith Laboratories.

$NbBr_4(PMe_2Ph)_3$, 1

PMe_2Ph (1.3 ml, 9.1 mmol) was added to a slurry of $NbBr_5$ (1.0 g, 2.0 mmol) in 40 ml of toluene. An orange precipitate was formed gradually and stirring was maintained for 1–2 days. Filtration afforded a dark red solution and orange solid (*ca.* 0.7 g). The solution was reduced in volume to about 5 ml, filtered again (very little insoluble material) and layered in a Schlenk tube with 20 ml of hexane. Dark red, crystalline $NbBr_4(PMe_2Ph)_3$ was obtained after two days. The liquid phase was decanted and the solid washed with hexane affording 1.15 g of the product (yield 70%).

$NbBr_3(PMe_2Ph)_3$, 2

PMe_2Ph (1.4 ml, 9.8 mmol) was added to a slurry of $NbBr_5$ (1.37 g, 2.77 mmol) in 15 ml of toluene. Sodium amalgam (0.065 g, 2.8 mmol of Na in 2.5 ml Hg) was added with stirring. Within 15 min the inital red color changed to green and after 30 min the solution was brown. This color sequence is identical to that observed during the sodium reduction of $NbCl_5$ in the presence of PMe_2Ph [1]. After two days the reaction mixture was filtered, concentrated to 5 ml and placed at −20 °C. Two days later 1.14 g (1.44 mmol, 52%) of red crystals of $NbBr_3(PMe_2Ph)_3 \cdot \frac{1}{2}C_7H_8$ were collected. Crystals of X-ray quality were grown by concentrating the reaction mixture to 10 ml and maintaining it at −20 °C for two days.

X-ray Crystallography

General procedures that have already been described elsewhere [14] were used to determine the crystal structures. The crystal parameters and basic

information about data collection and structure refinement are summarized in Table I. Polarization, Lorentz and absorption corrections were made to the measured intensities. In each case the metal atom position was obtained from a three-dimensional Patterson function. The remainder of the structure was determined by a subsequent series of difference Fourier syntheses and least squares refinements. In **2**, a molecule of toluene residing on a crystallographic inversion center was found to be disordered over two orientations. In the adopted disorder model the phenyl ring with fractional occupancy ½ is defined by the following sequence of atoms: C(40)′, C(41)′, C(42), C(43), C(44) and C(41), with C(45)′ being the methyl carbon atom bonded to C(40)′. Primed atoms are generated by the inversion center, which is located midway between the second and sixth C atoms in the toluene ring, C(41)′ and C(41), respectively. The fractional occupancy of all atoms is equal to ½, except C(41) for which it is equal to 1. Refinement of the structures was completed with anisotropic thermal parameters assigned to selected atoms (see Table II). Tables of structure factors and *B*s are available as supplementary material.

TABLE II. (a) Positional and Isotropic-Equivalent Thermal Parameters for $NbBr_4(PMe_2Ph)_3$.

Atom	*x*	*y*	*z*	*B* (A2)
Nb	0.1822(2)	0.10887(7)	−0.2971(2)	2.04(5)
Br(1)	0.0125(2)	0.1188(1)	−0.2361(4)	4.49(9)
Br(2)	0.3410(2)	0.1377(1)	−0.2545(3)	3.69(8)
Br(3)	0.2583(3)	0.0559(1)	−0.2110(4)	4.62(9)
Br(4)	0.2453(3)	0.1070(1)	−0.5444(3)	3.63(8)
P(1)	0.1421(6)	0.1690(2)	−0.3947(8)	2.7(2)
P(2)	0.0831(6)	0.0618(2)	−0.4231(8)	2.5(2)
P(3)	0.1853(6)	0.1180(2)	−0.0300(7)	2.9(2)
C(11)	0.239(2)	0.1922(7)	−0.461(2)	2.2(6)*[a]
C(12)	0.269(2)	0.1927(8)	−0.604(3)	2.6(7)*
C(13)	0.334(3)	0.211(1)	−0.645(3)	6(1)*
C(14)	0.384(2)	0.2322(9)	−0.564(3)	4.8(9)*
C(15)	0.360(2)	0.2314(8)	−0.427(3)	3.1(7)*
C(16)	0.293(2)	0.2137(9)	−0.380(3)	4.2(9)*
C(17)	0.087(2)	0.1990(7)	−0.282(3)	2.6(6)*
C(18)	0.057(2)	0.1691(8)	−0.536(3)	2.7(7)*
C(21)	0.004(2)	0.0369(8)	−0.315(3)	2.8(7)*
C(22)	−0.090(2)	0.0471(8)	−0.300(3)	2.9(7)*
C(23)	−0.143(2)	0.0290(9)	−0.211(3)	4.6(8)*
C(24)	−0.106(2)	0.0021(9)	−0.143(3)	3.3(8)*
C(25)	−0.015(2)	−0.0080(9)	−0.164(3)	4.0(8)*
C(26)	0.043(2)	0.0100(7)	−0.254(2)	2.6(6)*
C(27)	0.003(2)	0.0776(8)	−0.552(3)	3.5(8)*
C(28)	0.152(2)	0.0311(8)	−0.511(3)	3.7(8)*
C(31)	0.142(2)	0.1570(7)	0.028(2)	1.4(6)*
C(32)	0.207(2)	0.1831(8)	0.027(3)	3.8(8)*
C(33)	0.180(2)	0.2136(8)	0.066(3)	3.3(7)*
C(34)	0.084(2)	0.2194(8)	0.097(3)	4.1(8)*
C(35)	0.026(2)	0.1928(8)	0.102(3)	3.3(7)*
C(36)	0.051(2)	0.1619(8)	0.069(3)	3.5(8)*
C(37)	0.111(2)	0.0892(9)	0.058(3)	4.7(8)*
C(38)	0.296(2)	0.1115(8)	0.059(3)	3.8(7)*

(b) Positional and Isotropic-Equivalent Thermal Parameters for $NbBr_3(PMe_2Ph)_3 \cdot \frac{1}{2}C_7H_8$

Atom	*x*	*y*	*z*	*B* (A2)
Nb	0.43673(8)	0.23137(4)	0.15839(9)	2.77(2)
Br(1)	0.6905(1)	0.29006(6)	0.2538(1)	4.95(3)
Br(2)	0.4998(1)	0.17446(6)	−0.0963(1)	4.78(2)
Br(3)	0.2998(1)	0.27109(7)	0.3786(1)	5.59(3)
P(1)	0.1792(3)	0.1581(1)	0.0493(3)	3.56(6)
P(2)	0.4185(3)	0.3545(1)	0.0685(3)	3.65(6)
P(3)	0.5067(3)	0.1317(1)	0.3052(3)	3.52(5)
C(10)	0.0788(9)	0.2009(5)	−0.081(1)	3.5(2)
C(11)	0.122(1)	0.2054(5)	−0.225(1)	4.2(2)
C(12)	0.049(1)	0.2379(6)	−0.327(1)	4.7(2)
C(13)	−0.072(1)	0.2658(6)	−0.289(1)	5.4(3)
C(14)	−0.115(1)	0.2614(6)	−0.145(1)	5.6(3)
C(15)	−0.040(1)	0.2300(5)	−0.039(1)	4.9(3)
C(16)	0.055(1)	0.1345(6)	0.187(1)	5.5(3)
C(17)	0.180(1)	0.0709(5)	−0.064(1)	5.2(3)
C(20)	0.535(1)	0.3781(5)	−0.074(1)	3.7(2)
C(21)	0.490(1)	0.3572(6)	−0.227(1)	4.9(3)
C(22)	0.581(1)	0.3732(6)	−0.338(1)	5.8(3)
C(23)	0.715(1)	0.4107(6)	−0.296(1)	5.5(3)
C(24)	0.761(1)	0.4309(6)	−0.145(1)	5.9(3)
C(25)	0.671(1)	0.4146(5)	−0.034(1)	4.5(2)
C(26)	0.246(1)	0.3743(6)	−0.001(1)	5.7(3)
C(27)	0.471(1)	0.4267(5)	0.228(1)	5.2(3)
C(30)	0.373(1)	0.0593(5)	0.336(1)	3.5(2)
C(31)	0.291(1)	0.0691(5)	0.461(1)	4.5(2)
C(32)	0.186(1)	0.0151(6)	0.482(1)	5.8(3)
C(33)	0.160(1)	−0.0472(6)	0.382(2)	7.2(3)
C(34)	0.241(1)	−0.0572(6)	0.263(1)	6.3(3)
C(35)	0.349(1)	−0.0031(5)	0.241(1)	4.7(3)
C(36)	0.583(1)	0.1678(7)	0.498(1)	5.8(3)
C(37)	0.646(1)	0.0882(7)	0.222(1)	6.7(3)
C(40)	−0.063(3)	0.522(1)	0.456(3)	7.0(6)*[a]
C(41)	−0.021(2)	0.4589(9)	0.390(2)	10.7(5)*
C(42)	0.054(3)	0.413(1)	0.413(3)	7.4(7)*
C(43)	−0.120(4)	0.572(2)	0.461(4)	10(1)*
C(44)	−0.080(3)	0.495(2)	0.352(3)	8.2(7)*
C(45)	−0.131(3)	0.546(2)	0.368(4)	9.2(8)*

[a]Starred atoms were refined isotropically. Anisotropically refined atoms are given in the form of the isotropic equivalent thermal parameter defined as $4/3[a^2\beta_{11} + b^2\beta_{22} + c^2\beta_{33} + ab(\cos\gamma)\beta_{12} + ac(\cos\beta)\beta_{13} + bc(\cos\alpha)\beta_{23}]$.

Results and Discussion

Molecular Structures

The atomic positional parameters for **1** and **2** are listed in Table II, under (a) and (b), respectively. Bond distances and angles are presented in Tables III through VI. ORTEP drawings of the two molecules are shown in Figs. 1 and 2.

TABLE III. Bond Distances (Å) in $NbBr_4(PMe_2Ph)_3$.[a]

Nb–Br(1)	2.541(4)
Nb–Br(2)	2.604(4)
Nb–Br(3)	2.587(5)
Nb–Br(4)	2.621(4)
Nb–P(1)	2.721(10)
Nb–P(2)	2.709(9)
Nb–P(3)	2.683(8)
P(1)–C(11)	1.80(3)
P(1)–C(17)	1.84(3)
P(1)–C(18)	1.86(3)
P(2)–C(21)	1.88(3)
P(2)–C(27)	1.84(3)
P(2)–C(28)	1.83(3)
P(3)–C(31)	1.82(3)
P(3)–C(37)	1.82(3)
P(3)–C(38)	1.84(3)
C(11)–C(12)	1.49(4)
C(11)–C(16)	1.43(4)
C(12)–C(13)	1.27(5)
C(13)–C(14)	1.39(5)
C(14)–C(15)	1.40(4)
C(15)–C(16)	1.30(4)
C(21)–C(22)	1.41(4)
C(21)–C(26)	1.38(4)
C(22)–C(23)	1.38(4)
C(23)–C(24)	1.40(5)
C(24)–C(25)	1.38(5)
C(25)–C(26)	1.43(4)
C(31)–C(32)	1.43(4)
C(31)–C(36)	1.37(4)
C(32)–C(33)	1.37(5)
C(33)–C(34)	1.44(5)
C(34)–C(35)	1.37(5)
C(35)–C(36)	1.37(5)

[a]Numbers in parentheses are e.s.d.s in the least significant digits.

TABLE IV. Bond Angles (deg) in $NbBr_4(PMe_2Ph)_3$.[a]

Br(1)–Nb–Br(2)	136.5(2)
Br(1)–Nb–Br(3)	117.4(2)
Br(1)–Nb–Br(4)	124.0(2)
Br(1)–Nb–P(1)	74.7(2)
Br(1)–Nb–P(2)	73.9(2)
Br(1)–Nb–P(3)	75.9(2)
Br(2)–Nb–Br(3)	87.8(1)
Br(2)–Nb–Br(4)	82.2(1)
Br(2)–Nb–P(1)	80.1(2)
Br(2)–Nb–P(2)	149.4(2)
Br(2)–Nb–P(3)	76.1(2)
Br(3)–Nb–Br(4)	98.0(2)
Br(3)–Nb–P(1)	167.2(2)
Br(3)–Nb–P(2)	76.8(2)
Br(3)–Nb–P(3)	77.5(2)
Br(4)–Nb–P(1)	76.5(2)
Br(4)–Nb–P(2)	74.1(2)
Br(4)–Nb–P(3)	158.0(2)
P(1)–Nb–P(2)	112.0(3)
P(1)–Nb–P(3)	103.2(3)
P(2)–Nb–P(3)	124.5(3)
Nb–P(1)–C(11)	117(1)
Nb–P(1)–C(17)	119(1)
Nb–P(1)–C(18)	114(1)
C(11)–P(1)–C(17)	101(1)
C(11)–P(1)–C(18)	103(1)
C(17)–P(1)–C(18)	100(1)
Nb–P(2)–C(21)	116(1)
Nb–P(2)–C(27)	113(1)
Nb–P(2)–C(28)	116(1)
C(21)–P(2)–C(27)	102(1)
C(21)–P(2)–C(28)	103(2)
C(27)–P(2)–C(28)	104(1)
Nb–P(3)–C(31)	115.7(9)
Nb–P(3)–C(37)	112(1)
Nb–P(3)–C(38)	118(1)
C(31)–P(3)–C(37)	103(1)
C(31)–P(3)–C(38)	106(1)
C(37)–P(3)–C(38)	100(2)
P(1)–C(11)–C(12)	125(2)
P(1)–C(11)–C(16)	123(2)
C(12)–C(11)–C(16)	112(3)
C(11)–C(12)–C(13)	122(3)
C(12)–C(13)–C(14)	124(3)
C(13)–C(14)–C(15)	115(3)
C(14)–C(15)–C(16)	123(3)
C(11)–C(16)–C(15)	124(3)
P(2)–C(21)–C(22)	118(2)
P(2)–C(21)–C(26)	116(2)
C(22)–C(21)–C(26)	126(3)
C(21)–C(22)–C(23)	115(3)
C(22)–C(23)–C(24)	122(3)
C(23)–C(24)–C(25)	122(3)
C(24)–C(25)–C(26)	119(3)
C(21)–C(26)–C(25)	117(3)
P(3)–C(31)–C(32)	116(2)
P(3)–C(31)–C(36)	123(2)
C(32)–C(31)–C(36)	121(3)
C(31)–C(32)–C(33)	121(3)
C(32)–C(33)–C(34)	119(3)
C(33)–C(34)–C(35)	117(3)
C(34)–C(35)–C(36)	125(3)
C(31)–C(36)–C(35)	117(3)

[a]Numbers in parentheses are e.s.d.s in the least significant digits.

$NbBr_4(PMe_2Ph)_3$, I

This molecule is geometrically similar to the seven-coordinate PMe_3 adducts of Nb(IV) and Ta(IV) chlorides and to the PMe_2Ph adducts of Mo(IV) halides [15, 16]. It is a seven-coordinate, capped octahedron with virtual C_{3v} symmetry. As in other compounds with this geometry the unique halide atom, Br(1), caps the P_3 face and is closer to the central metal atom than are the other bromide ligands. The comparison of average interatomic dimensions in the MX_4L_3 complexes idealized to C_{3v} symmetry is presented in Table VII. The metal–

TABLE V. Bond Distances (Å) in $NbBr_3(PMe_2Ph)_3 \cdot \frac{1}{2}C_7H_8$.[a]

Nb–Br(1)	2.573(1)
Nb–Br(2)	2.562(1)
Nb–Br(3)	2.554(1)
Nb–P(1)	2.716(2)
Nb–P(2)	2.647(3)
Nb–P(3)	2.619(3)
P(1)–C(10)	1.825(9)
P(1)–C(16)	1.833(10)
P(1)–C(17)	1.862(9)
P(2)–C(20)	1.817(9)
P(2)–C(26)	1.838(10)
P(2)–C(27)	1.854(9)
P(3)–C(30)	1.826(9)
P(3)–C(36)	1.840(10)
P(3)–C(37)	1.840(10)
C(10)–C(11)	1.396(12)
C(10)–C(15)	1.408(12)
C(11)–C(12)	1.385(13)
C(12)–C(13)	1.397(14)
C(13)–C(14)	1.39(2)
C(14)–C(15)	1.408(15)
C(20)–C(21)	1.401(13)
C(20)–C(25)	1.392(13)
C(21)–C(22)	1.409(13)
C(22)–C(23)	1.38(2)
C(23)–C(24)	1.38(2)
C(24)–C(25)	1.410(14)
C(30)–C(31)	1.418(12)
C(30)–C(35)	1.368(12)
C(31)–C(32)	1.386(14)
C(32)–C(33)	1.39(2)
C(33)–C(34)	1.38(2)
C(40)′–C(41)′	1.43(4)
C(40)′–C(41)	1.52(3)
C(40)′–C(45)′	1.18(4)
C(41)′–C(42)	1.25(3)
C(41)–C(44)	1.03(4)
C(42)–C(43)	1.23(4)
C(43)–C(44)	1.79(5)

[a]Numbers in parentheses are e.s.d.s in the least significant digits.

TABLE VI. Bond Angles (deg) in $NbBr_3(PMe_2Ph)_3 \cdot \frac{1}{2}C_7H_8$.[a]

Br(1)–Nb–Br(2)	95.36(4)
Br(1)–Nb–Br(3)	101.81(4)
Br(1)–Nb–P(1)	174.51(7)
Br(1)–Nb–P(2)	83.49(6)
Br(1)–Nb–P(3)	82.28(6)
Br(2)–Nb–Br(3)	162.82(5)
Br(2)–Nb–P(1)	80.84(6)
Br(2)–Nb–P(2)	94.68(6)
Br(2)–Nb–P(3)	94.36(6)
Br(3)–Nb–P(1)	82.08(6)
Br(3)–Nb–P(2)	86.70(6)
Br(3)–Nb–P(3)	88.63(6)
P(1)–Nb–P(2)	100.70(8)
P(1)–Nb–P(3)	94.02(8)
P(2)–Nb–P(3)	163.78(8)
Nb–P(1)–C(10)	114.8(3)
Nb–P(1)–C(16)	117.2(3)
Nb–P(1)–C(17)	115.6(3)
C(10)–P(1)–C(16)	104.2(5)
C(10)–P(1)–C(17)	101.6(4)
C(16)–P(1)–C(17)	101.3(5)
Nb–P(2)–C(20)	115.0(3)
Nb–P(2)–C(26)	120.1(4)
Nb–P(2)–C(27)	110.5(4)
C(20)–P(2)–C(26)	104.6(5)
C(20)–P(2)–C(27)	103.8(4)
C(26)–P(2)–C(27)	100.9(5)
Nb–P(3)–C(30)	120.3(3)
Nb–P(3)–C(36)	111.0(4)
Nb–P(3)–C(37)	113.0(4)
C(30)–P(3)–C(36)	102.6(5)
C(30)–P(3)–C(37)	104.3(5)
C(36)–P(3)–C(37)	104.0(6)
P(1)–C(10)–C(11)	119.2(7)
P(1)–C(10)–C(15)	121.3(8)
C(11)–C(10)–C(15)	119.5(9)
C(10)–C(11)–C(12)	120.6(9)
C(11)–C(12)–C(13)	121(1)
C(12)–C(13)–C(14)	118(1)
C(13)–C(14)–C(15)	121(1)
C(10)–C(15)–C(14)	119(1)
P(2)–C(20)–C(21)	119.9(7)
P(2)–C(20)–C(25)	121.2(8)
C(21)–C(20)–C(25)	118.9(9)
C(20)–C(21)–C(22)	120.2(9)
C(21)–C(22)–C(23)	120(1)
C(22)–C(23)–C(24)	120(1)
C(23)–C(24)–C(25)	120(1)
C(20)–C(25)–C(24)	120(1)
P(3)–C(30)–C(31)	118.7(7)
P(3)–C(30)–C(35)	121.2(7)
C(31)–C(30)–C(35)	120.1(9)
C(30)–C(31)–C(32)	119(1)
C(31)–C(32)–C(33)	121(1)
C(32)–C(33)–C(34)	120(1)
C(33)–C(34)–C(35)	119(1)
C(30)–C(35)–C(34)	121(1)
C(40)′–C(41)–C(44)	119(3)
C(41)′–C(40)′–C(45)′	111(4)
C(41)–C(40)′–C(45)′	142(4)
C(41)–C(40)′–C(41)′	106(2)
C(40)′–C(41)′–C(42)	144(3)
C(41)′–C(42)–C(43)	111(3)
C(42)–C(43)–C(44)	114(4)
C(41)–C(44)–C(43)	127(4)

[a]Numbers in parentheses are e.s.d.s in the least significant digits.

chloride distances for Mo, Nb and Ta are practically identical. The metal–bromide bond lengths are about 0.11–0.15 Å longer than the corresponding M–Cl distances which is consistent with the relative co-

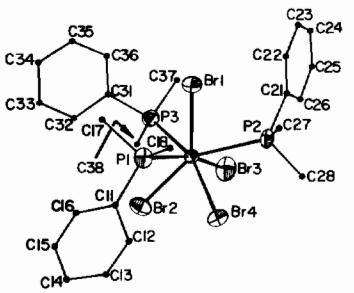

Fig. 1. An ORTEP drawing of the $NbBr_4(PMe_2Ph)_3$ molecule. Thermal ellipsoids are drawn at 50% probability level. Carbon atoms were assigned arbitrarily small thermal parameters for the sake of clarity.

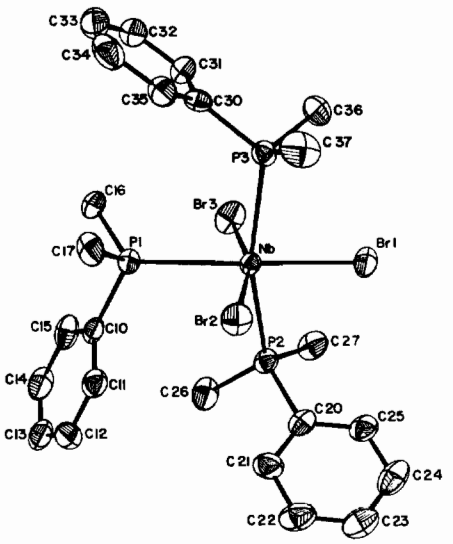

Fig. 2. An ORTEP drawing of the $NbBr_3(PMe_2Ph)_3$ molecule. Thermal ellipsoids are drawn at 35% probability level.

valent radii of Cl and Br, 0.99 Å and 1.14 Å [17], respectively. We would suggest that there is an error in the reported value of the $M-X_c$ distance for $MoBr_4(PMe_2Ph)_3$; it is egregiously out of line with the M–X bond length pattern in all the other compounds in Table VII. We also note that the Nb–P distance in **1**, 2.704[11] Å, is very long compared to that in its molybdenum analog, 2.580(7) Å. This is the same kind of relationship, but to an even greater degree, as that seen in the three chloro compounds where the group V M–P distances, 2.651[6] Å and 2.640[6] Å, are quite a lot longer than the Mo–P distance, even though the corresponding M–X distances are virtually the same whether the metal atom is Nb, Ta or Mo. We shall return to this question of M–P distance variations later. The structures of two other dimethylphenylphosphine adducts of group V halides are known, but neither is of the seven-coordinate, capped-octahedron type. $TaCl_4(PMe_2Ph)_2$ has a distorted *cis*-octahedral structure [2b] and $Nb_2Cl_8(PMe_2Ph)_4$ is a dimer of square antiprisms [1]. Crystals of both of these compounds were grown from solutions with excess phosphine present. Experimental data indicate that in solution several species exist in a complex equilibrium. We feel that the reason compounds of different geometries are isolated from solutions differing either in the metal or halide present is not an inherent preference by one combination of metal and halide for a certain geometry; instead, we attribute it to the differences in relative solubilities of these compounds, with slightly different solvent combinations and substrate concentrations favoring the crystallization of different compounds.

$NbBr_3(PMe_2Ph)_3$, 2

The molecule is essentially octahedral with a meridional disposition of the ligands. The deviation of angles from 90° is attributable to repulsions within

TABLE VII. A Comparison of Bond Distances (Å) and Bond Angles (deg) in Phosphine Adducts of the Type MX_4L_3.[a,b]

	$NbBr_4(PMe_2Ph)_3$	$MoBr_4(PMe_2Ph)_3$	$NbCl_4(PMe_3)_3$	$MoCl_4(PMe_2Ph)_3$[c]	$TaCl_4(PMe_3)_3$
$M-X_c$	2.541(4)	2.425(7)	2.409(4)	2.399(3)	2.417(3)
M–X	2.604[10]	2.560(5)	2.453[13]	2.448[5]	2.447[8]
M–P	2.704[11]	2.580(7)	2.651[6]	2.577[3]	2.640[6]
X_c-M-X	126[6]	127.4(1)	125[4]	127.2	126[5]
$X-M-P_{cis}$	76.9[8]	77.3[8]	76.9[7]		76.8[6]
$X-M-P_{trans}$	158[5]	158.0(2)	159[4]		159[4]
P–M–P	113[6]	113.2(2)	113[3]		113[4]
X_c-M-P	74.8[6]	74.5(2)	74.9[5]	74.6	74.8[6]
X–M–X	89[4]	86.9(2)	89(3)		88[3]
Reference	This work	15	3	16	2

[a]Numbers in brackets are variances, obtained from the expression $[\Sigma\Delta_i^2/n(n-1)]^{1/2}$, where Δ_i is the deviation of the ith value from the arithmetic mean and n is the total number of values averaged. [b]X_c–halide capping the octahedron. [c]Incomplete set of bond angles available.

TABLE VIII. A Comparison of Some Interatomic Dimensions in the Molecules of the Type *mer*-$MX_3(PMe_2Ph)_3$.[a,b]

	X = Br		X = Cl	
	Nb(d^2)	Rh(d^6)	Ir(d^6)[c]	Tc(d^4)[c]
M–X (*trans* X)	2.558[4]	2.499[23]	2.364[2]	2.33[0]
M–X (*trans* P)	2.573(1)	2.568(2)	2.436[3]	2.45[1]
M–P (*trans* P)	2.633[14]	2.391[8]	2.373[5]	2.47[1]
M–P (*trans* X)	2.716(2)	2.296(3)	2.280[2]	2.42[0]
X–M–X *trans*	162.82(5)	177.5(1)	176.23[32]	177.0[1]
P–M–P *trans*	163.78(8)	166.8(1)	166.55[4]	167.3[1]
Reference	This work	19	20	21

[a]For data concerning Re, Os and Ir complexes see ref. 18, where a similar comparison has been made. [b]Numbers in brackets are variances, calculated as defined in footnote a in Table VII, or mean e.s.d., whichever is larger. [c]Two independent molecules per asymmetric unit.

the P_3 and Br_3 triangles. Turning now to bond lengths, we find that the niobium complex is unique among species of the type $MX_3(PMe_2Ph)_3$, where X = Cl or Br, for which crystallographic data are available [18–21] (see Table VIII). In all previously described compounds the following patterns of metal–ligand bond lengths are observed: (a) M–X *trans* to P is longer than M–X *trans* to X, and (b) M–P *trans* to P is longer than M–P *trans* to X. These differences in bond lengths are quite significant and can be attributed to a *trans* influence of the phosphorus atoms which exceeds that of the X atoms. In $NbBr_3(PMe_2Ph)_3$ lengthening of the Nb–Br bond *trans* to P is only slight and the relative lengths of non-equivalent Nb–P bonds are reversed. Moreover, the Nb–P bonds of both types appear to be surprisingly long as compared to those in the other three compounds. No simple steric argument seems able to account for any of these unusual properties of the niobium compound since niobium(III), being the largest of the four metal atoms, should be least crowded.

It appears that the affinity of phosphine ligands for the group V metal atoms, at least in their oxidation states III and IV, is low. Since the M–P bonds are weak, they do not exert a *trans* influence. In compound **1** reported in this paper, as in a host of other phosphine derivatives whose structures have been previously described, the Nb–P and Ta–P bonds are also very long in comparison to metal–halogen bonds. This major difference between the group V metal atoms and those to the right (even those in group VI) may have its causes in the energy and diffuseness of the d orbitals and also the small number of d electrons, but a simple qualitative explanation does not seem immediately obvious.

Chemical Properties and Magnetic Resonance Spectra

The ability of phosphines to reduce metal halides is well recognized [22]. Nonetheless, we had not anticipated this in the case of $NbBr_5$ since it had not been observed with $NbCl_5$. It is, however, the dominant process since the only product we have isolated, in about 70% yield based on $NbBr_5$, is the niobium(IV) species $NbBr_4(PMe_2Ph)_3$.

The elemental analysis of compound **2** gave low values for the non-metallic elements, but this is a not uncommon problem in the chemistry of niobium and tantalum [23]. The molar ratio of P to Br was close to unity, suggesting that little or no niobium(IV) species were present.

Both **1** and **2** are expected to be paramagnetic with one and two unpaired electrons respectively. Their EPR spectra in CH_2Cl_2 solution and glass were measured and are shown in Figs. 3 and 4. $NbBr_4(PMe_2Ph)_3$ shows a very weak and broad signal at room temperature. Upon cooling to −196 °C the signal becomes about 250 times more intense and coupling to ^{93}Nb (S = 9/2, 10 lines, $\langle g \rangle = 1.87$, $\langle A \rangle$ = 185 G) is observed. No superhyperfine coupling to phosphorus nuclei is resolved.

The solution obtained by dissolution of $NbBr_3(PMe_2Ph)_3$ gives a well resolved and to a certain extent symmetric EPR signal at room temperature. This, although somewhat surprising for a d^2 high

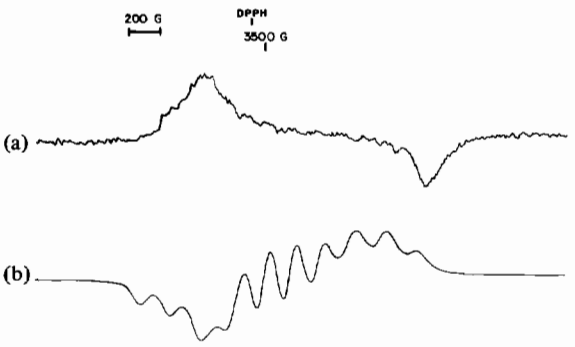

Fig. 3. EPR spectra of CH_2Cl_2 solution of $NbBr_4(PMe_2Ph)_3$. (a) at room temperature; (b) at −196 °C; the low temperature spectrum, (b), is about 250 times more intense than (a).

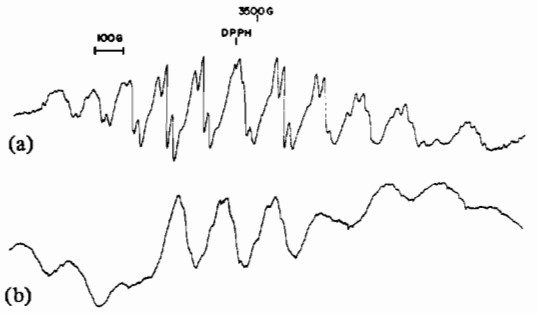

Fig. 4. EPR spectra of CH_2Cl_2 solution of $NbBr_3(PMe_2Ph)_3 \cdot \frac{1}{2}C_7H_8$. (a) at room temperature; (b) at −196 °C; the intensity ratio (b) to (a) is about 8:1; the former is about 25 times less intense than low temperature signal for $NbBr_4(PMe_2Ph)_3$.

spin system, is not in fact unprecedented. Several $M(d^2)$, M = Nb and Ta, monomeric complexes have been reported to give well resolved EPR spectra [8, 11]. While it is possible that in these systems there really are unusually favorable conditions for paramagnetic resonance we believe that caution must be exercised before any definite conclusions are drawn. It seems quite possible that these good EPR signals may be attributable to some M(IV) impurities or decomposition products. Factors pointing to that possibility, are first, the 'molar' intensity of the resonance of $NbBr_3(PMe_2Ph)_3$ is much weaker than those observed for pure $Nb(d^1)$ complexes, *e.g.*, $NbCl_2(dpm)_2$ [24]*. Second, lowering of the temperature to −196 °C results in a significantly less resolved spectrum, which suggests the species giving the room temperature signal are different from those in the glass. High sensitivity of Nb and Ta in the +3 oxidation state towards oxidants makes it almost impossible to avoid traces of oxidized species in samples.

In addition, the spectrum in part (a) of Fig. 4 has two features that are inconsistent with simply assigning it to molecules of compound 2. There is an 'extra' component, presumably the one to the extreme right. In addition the super-hyperfine appears to consist of triplets rather than quartets.

In general EPR spectroscopy of low-valent Nb and Ta complexes is far from a routine tool. A number of well behaved systems have been reported, such as *trans*-$MCl_4(phosphine)_2$ complexes [2, 6], M(IV) hydrides [10] and some MX_4L_2 species [25]. However our experience with the $MCl_4(phosphine)_n$ complexes indicates that in many cases inconclusive or difficult to interpret results are obtained. This is exemplified [3] by $NbCl_4(PMe_3)_4$ and $NbCl_4(PMe_3)_3$ which give, in terms of intensity and resolution, very good and very poor EPR signals, respectively. Additional complications may well arise from equilibria between several species in solution. In summary, meaningful interpretation of all EPR spectra of complexes in the class under discussion will not really be possible until a comprehensive study of the subject is carried out.

^{31}P NMR spectra show that $NbBr_3(PMe_2Ph)_3$ does not dimerize in solution to a significant extent, since dimers should be diamagnetic and hence NMR active. The spectrum of the post-reaction solution containing excess ligand has only one signal at −32 ppm. This signal, attributed to free PMe_2Ph, is shifted with respect to the pure phosphine (+47 ppm) [26] due to the presence of the paramagnetic complex. The spectrum of $NbBr_3(PMe_2Ph)_3$ dissolved in CH_2Cl_2 is featureless, indicating neither appreciable formation of a diamagnetic dimer nor detectable dissociation of the ligand. This contrasts with the behavior of $TaCl_3(PMe_3)_3$, which dimerizes readily to $Ta_2Cl_6(PMe_3)_4$ in the absence of excess phosphine [8]. The stability of the Nb(III) complex is consistent with the greater size of the ligands. IR spectra and lack of color change show that even at 2000 psi. $NbBr_3(PMe_2Ph)_3$ is inert towards H_2, while at much lower pressures $TaCl_3(PMe_3)_3$ reacts [8] with H_2 to form $Ta_2Cl_6H_2(PMe_3)_4$ [13]. These observations support the hypothesis put forward by Schrock [8] that oxidative addition of H_2 in this case is associated with the presence of a metal–metal bond and is not a general property of Nb(III) and Ta(III) complexes.

*dpm represents the $Me_3CC(O)CHC(O)CMe_3^-$ ion.

Acknowledgements

We are greateful to Dr. Austin H. Reid, Jr. for running the high pressure reaction of 2 with H_2. We thank the Robert A. Welch Foundation for support under Grant No. A-494. M.P.D. is a National Science Foundation Predoctoral Fellow and also holds a Texaco-IUCCP Fellowship from this department.

Supplementary Material Available

Tables of structure factors and anisotropic thermal parameters (25 pages) are available from the authors.

References

1 F. A. Cotton and W. J. Roth, *Inorg. Chem., 23,* 945 (1984).
2 F. A. Cotton, S. A. Duraj and W. J. Roth, *Inorg. Chem., 23,* 3592(a) 4046(b) (1984).
3 F. A. Cotton, M. P. Diebold and W. J. Roth, *Polyhedron,* in press.

4 P. D. W. Boyd, T. C. Jones, C. E. F. Nielson and C. E. F. Richard, *J. Chem. Soc., Chem. Commun.*, 1086 (1984).
5 L. E. Manzer, *Inorg. Chem., 16,* 525 (1977).
6 (a) E. Samuel, G. Labauze and J. Livage, *Nouv. J. Chim., 1,* 93 (1977);
(b) G. Labauze, E. Samuel and J. Livage, *Inorg. Chem., 19,* 1384 (1980).
7 (a) F. A. Cotton and W. J. Roth, *Inorg. Chem., 22,* 3654 (1983);
(b) F. A. Cotton, S. A. Duraj and W. J. Roth, *Acta Crystallogr., Sect. C:,* in press.
8 S. M. Rocklage, H. W. Turner, J. D. Fellmann and R. R. Schrock, *Organometallics, 1,* 703 (1982).
9 A. P. Sattelberger, R. B. Wilson and J. C. Huffman, *Inorg. Chem., 21,* 2392 (1982).
10 M. L. Luetkens, W. L. Elcesser, J. C. Huffman and A. P. Sattelberger, *Inorg. Chem., 23,* 1718 (1984).
11 M. E. Clay and T. M. Brown, *Inorg. Chim. Acta, 58,* 1 (1982).
12 F. A. Cotton, S. A. Duraj and W. J. Roth, *J. Am. Chem. Soc., 106,* 4749 (1984) and refs. therein.
13 A. P. Sattelberger, R. B. Wilson and J. C. Huffman, *Inorg. Chem., 21,* 4179 (1982).
14 A. Bino, F. A. Cotton and F. E. Fanwick, *Inorg. Chem., 18,* 3558 (1979).
15 M. G. B. Drew, J. D. Wilkins and A. P. Wolters, *J. Chem. Soc., Chem. Commun.*, 1278 (1972).
16 L. Manojlovic-Muir, *Inorg. Nucl. Chem. Lett., 9,* 59 (1973).
17 F. A. Cotton and G. Wilkinson, 'Advanced Inorganic Chemistry', Wiley, New York, 1980, p. 543.
18 L. Aslanov, R. Mason, A. G. Wheeler and P. O. Whimp, *J. Chem. Soc., Chem. Commun.*, 30 (1970).
19 R. B. English, *Cryst. Struct. Commun., 8,* 167 (1979).
20 G. B. Robertson and P. A. Tucker, *Acta Crystallogr., Sect. B:, 37,* 814 (1983).
21 G. Bandoli, D. A. Clemente and U. Mazzi, *J. Chem. Soc., Dalton Trans.*, 125 (1976).
22 C. A. McAuliffe and W. Levason, 'Phosphine, Arsine and Stibine Complexes of the Transition Elements', Elsevier, Amsterdam, 1979, p. 38.
23 A. J. Benton, M. G. B. Drew, R. J. Hobson and D. A. Rice, *J. Chem. Soc., Dalton Trans.*, 1304 (1981).
24 F. A. Cotton, M. P. Diebold and W. J. Roth, *Polyhedron,* in press.
25 D. A. Miller and R. D. Bereman, *Coord. Chem. Rev., 9,* 107 (1972/73).
26 G. M. Kosolapoff, 'Organic Phosphorus Compounds, Vol. 1', Wiley, New York, 1972.